AJAE

Open Access

Vol. 14, No. 4, pp. 335-344, December 2020
doi: https://doi.org/10.5572/ajae.2020.14.4.335
ISSN (Online) 2287-1160, ISSN (Print) 1976-6912

Research Article

Visibility Degradation and Its Contributors at an Urban Site in Korea

Chang-Jin Ma*, Cheol-Soo Lim[1)], Gong-Unn Kang[2)], Sun-A Jung[1)], Mi-Ra Jo[1)]

Department of Environmental Science, Fukuoka Women's University, Fukuoka 813-8529, Japan
[1)]Department of Air Quality Research, National Institute of Environmental Research, Incheon 22689, Republic of Korea
[2)]Department of Medical Administration, Wonkwang Health Science University, Iksan 54538, Republic of Korea

***Corresponding author.**
Tel: +81-90-9470-9293
E-mail: ma@fwu.ac.jp

Received: 17 February 2020
Revised: 23 March 2020
Accepted: 8 July 2020

ABSTRACT In order to provide a better knowledge of visibility degradation during the $PM_{2.5}$ event day (episodic high $PM_{2.5}$ level, hereafter called as "event day"), the relationship between visibility and the chemical species of $PM_{2.5}$ measured in Gwangju, Korea was estimated. Moreover, a visibility forecasting model was constructed by a statistical approach. The diurnal variation of visibility and $PM_{2.5}$ concentration on the event day indicated that as the concentration of $PM_{2.5}$ increased, more light was absorbed and scattered, resulting in visibility deterioration. The averaged visibility during the event day was 7.9 km, which was almost three times lower than that observed during a non-event day. Although the hygroscopic growth of aerosol was not considered in this study, it has been proved that NH_4NO_3 and organics dominantly contributed to the light scattering during the $PM_{2.5}$ event day in Gwangju, Korea. The visibility determined in this study had also a negative correlation with PM_{10}, nitrate, relative humidity, EC, OC, and sulfate. Meanwhile, visibility was positively linked with wind speed and temperature. The results of interrelationship and a multiple regression model suggest that among the meteorological variables, temperature was the main variable that influenced visibility.

KEY WORDS $PM_{2.5}$, Visibility, Chemical composition, Light scattering, Nephelometer, Regression model

1. INTRODUCTION

Fine particles, especially those with diameter 2.5 micrometers or less (generally called as $PM_{2.5}$), are believed to be the main cause of reduced visibility. When $PM_{2.5}$ in the atmosphere scatters light, haze is caused and reduces the distance people can see and obscures the color and clarity of the objects. Visibility of less than 100 m is usually reported as zero. In this condition, roads and airports may be closed. Due to repeatedly poor visibility at many airports around the world, sometimes flights are delayed or cancelled.

Visibility degradation is mainly caused by the absorption and scattering of light by particles and gases. The field observation by Kim *et al.* (2008) suggested that the light scattering by particles accounted for 52.8 to 81.3% of the worsening of visibility at the urban site of Gwangju, Korea. Among various $PM_{2.5}$ components, major four kinds are the most effective at reducing visibility. They are sulfates,

nitrates, organic carbon (OC), and elemental carbon (EC, also called as BC (Black Carbon)) (Sloane *et al.*, 1991).

The contribution of aerosol components to the light-scattering varies according to the region. Wang *et al.* (2015) reported that the apportionment contributions from organic, sulfate, ammonium nitrate and ammonium chloride were 54%, 24%, 12%, and 10%, respectively in Beijing, China during a wintertime intense haze episode. They also mentioned that the organic components contributed greatly to the light extinction (about 45% in Shenzhen, China (Yao *et al.*, 2010) and 9–50% in the Eastern USA (Watson, 2002)) by quoting other research papers.

It is significantly meaningful to study visibility based on the chemical compositions of aerosol obtained through a real-time chemical analysis. However, the real-time or quasi-real-time monitored chemical compositions of $PM_{2.5}$ have seldom been applied.

In the present study, the relationship between visibility and the simultaneously measured chemical composition of $PM_{2.5}$ was estimated. Moreover, the simplified visibility forecasting model was constructed by a statistical approach based on the routinely monitored $PM_{2.5}$ and meteorological parameters. If visibility can be easily forecasted through the routinely monitored data, we can protect ourselves from various risks of our health and our daily lives.

2. EXPERIMENTAL METHODS

2.1 Description of the Monitoring Site

Gwangju Metropolitan City, the sixth largest city in South Korea, is located in between a mountainous area in the east and a plains area of the southwestern part of the Korean Peninsula. Gwangju has a population of 1.49 million people over an area of 501.2 km^2. The annual average temperature is 15°C and the highest average is 33.1°C in August.

As a major source of air pollution, about 636,743 motor vehicles including 92,396 heavy duty are registered in Gwangju (The car registration number by year, 2016). The main industries of Gwangju are automobile, home appliances, high-tech components, semiconductor, and cultural contents.

Monitoring was carried out on the roof of a three-story building (13.5 m) of the Honam area air pollution intensive monitoring site (35.23N; 126.85E). The surroundings of this monitoring site are education and research facilities, and residential and commercial areas with some minor point sources such as electronic manufactories and precision machinery industries. Six-lane roads, usually with light traffic, are located 50 m all around the monitoring site.

2.2 Instruments and Measurements

The hourly data of the ionic species in $PM_{2.5}$ were directly obtained using the URG-9000D Ambient Ion Monitor (AIM, URG Co.). AIM has an additional ion detector to allow for time-resolved direct measurements of both cations and anions. $PM_{2.5}$ is drawn into the AIM Monitor through a $PM_{2.5}$ sharp-cut cyclone and then the sample is drawn through a Liquid Diffusion Denuder. $PM_{2.5}$ laden air stream next enters the Aerosol Super-Saturation Chamber to enhance particle growth. The enlarged particles in the An Inertial Particle Separator are then injected into the Ion Chromatograph. Ion Chromatography (IC) (ICS-2000, Dionex Co.) was used to determine the concentrations of various ions present in $PM_{2.5}$. Before running the collected PM samples, the IC system was calibrated using each standard solution. By comparing the data obtained from the PM samples to those obtained from the known standard solutions, the ionic species of PM samples could be identified and quantitated. Samples were analyzed for ammonium, nitrate, and sulfate. Detection limits of ammonium, nitrate, and sulfate are 0.339, 0.020, and 0.023 $\mu g/m^3$, respectively.

The comparison study between the filter-based laboratory IC technique and AIM method conducted by Beccaceci *et al.* (2015) showed an overall good correlation ($R^2 > 0.83$) for ammonium, nitrate, and sulfate.

The concentration of OC and EC in $PM_{2.5}$ collected on the quartz filters for 45 minutes with a flow rate of 8 lpm was determined using the thermal-optical transmittance (TOT) method. TOT method was designed for the analysis of the carbonaceous fraction of particulate diesel exhaust based on the National Institute of Occupational Safety and Health method 5040 (NIOSH 5040) (Karanasiou *et al.*, 2015). In order to estimate the carbon of the blank filter contaminated during handling and transport, the laboratory blank filters were also analyzed in the same way as samples. Carbon dioxide produced in the analytical procedure of OC and EC was measured by the Non-Dispersive Infra-Red (NDIR) detectors that are the industry standard method of measuring the concen-

tration of carbon oxides (CO and CO_2). The limit of detections (LODs) of OC and EC were calculated as 0.65 and 0.02 μg/m^3, respectively. Karanasiou *et al.* (2015) gave a full detail of TOT method.

In order to measure a highly variable light-scattering coefficient, the three-wavelength (i.e., 450 nm (blue), 550 nm (green), and 700 nm (red)) Integrating Nephelometer with backscatter shutter (Model 3563, TSI Scientific Inc., USA) was applied. This unique instrument is one of well-known excellent devices for the measurement of short-term measurements of the light-scattering coefficient of ambient particles. Sensitivity to light-scattering coefficients is as low as 2.0×10^{-7} per meter (60-second averaging time) (Anderson and Ogren, 1998). Integrating Nephelometers measure the angular integral of light scattering that yields the quantity called the scattering coefficient, which is used in the Beer-Lambert Law to calculate total light extinction (Bodhaine *et al.*, 1991).

Light-absorption coefficient of particles was measured by the Aethalometer (Magee Scientific Inc., USA). The aethalometer is the earliest and most common method used for a real-time readout of the concentration of BC in an air stream. Aethalometers are now constructed to perform their optical analyses simultaneously at multiple wavelengths, typically spanning the range from 370 nm (near-ultraviolet) to 950 nm (near-infrared). The Aethalometer collects the sample on a quartz fiber filter tape, and performs a continuous optical analysis, while the sample is collecting (Hansen *et al.*, 1982).

All monitoring and measurement instruments were intensively operated from May 26 to June 15, 2016.

2. 3 Determination of Visibility

Visibility is generally described as the maximum horizontal distance at which a target with a sky background can be visually observed by our eyes. As the early theory of visibility, Koschmieder (1924) developed below formula (i.e., Koschmieder's formula).

$$Visibility\ (\text{km}) = 3.912/\sigma_{ext}$$

where σ_{ext} is extinction coefficient and it is the total attenuation of visible radiation due to scattering and absorption by gas molecules, aerosols, and other components (e.g. fog and cloud droplets) in the atmosphere.

The σ_{ext} may be divided into a scattering coefficient, σ_{scat} and an absorption coefficient, σ_{abs}:

$$\sigma_{ext} = \sigma_{scat} + \sigma_{abs}.$$

The scattering and absorption coefficients may therefore be further subdivided into

$$\sigma_{scat} = \sigma_{sg} + \sigma_{sp} \text{ and } \sigma_{abs} = \sigma_{ag} + \sigma_{ap}.$$

Therefore, σ_{ext} is ultimately composed as follows.

$$\sigma_{ext} = \sigma_{sg} + \sigma_{sp} + \sigma_{ag} + \sigma_{ap}.$$

where the subscripts of *s*, *a*, *g*, and *p* denote scattering, absorption, due to gas molecules, and due to PM, respectively.

The σ_{sg}, i.e., scattering due to gas molecules is also called 'Rayleigh scattering'. It was calculated by Rayleigh scattering efficiency 0.12×10^{-4}/m (Malm *et al.*, 1996). The σ_{ag} was determined by $3.3 \times NO_2$ concentration (ppm) $\times 10^{-4}$ (Malm *et al.*, 1994). The σ_{sp} was directly measured by a Nephelometer. The σ_{ap} could be calculated by multiplying the BC concentration (ng/m^3) measured by Aethalometer by a factor of 8.28 m^2/g. The conversion factor of 8.28 m^2/g used in this study was applied in Beijing previously by Yan *et al.* (2008) and He *et al.* (2009).

2. 4 Concept of Multivariate Analysis for Visibility Forecast

A multiple regression analysis was applied to the visibility forecasting. It can be performed based on the relationship between multiple explanatory variables and a response variable by fitting a linear equation as follows:

$$Y_i = C_0 + C_1x_1 + \ldots + C_4x_4 + e$$

where Y_i, $C_{0\text{-}4}$, $x_{1\text{-}4}$, and e are response variable (visibility), constants, explanatory variables ($PM_{2.5}$, temperature, wind speed, and relative humidity), and random error, respectively.

3. RESULTS AND DISCUSSION

3. 1 Diurnal Variation of Visibility and $PM_{2.5}$

Photo 1 shows the surrounding from the ground station of this study on a non-event day (a clean day with the $PM_{2.5}$ concentration of 21 μg/m^3) (top) and the event day when $PM_{2.5}$ reached 63 μg/m^3 (bottom). As shown in the photo, it is possible to find out the clear difference between two scenic views.

The diurnal variations of visibility on the event day and a non-event day are drawn in Fig. 1. Visibility shows

obvious diurnal variations on both the event day and a non-event day. The diurnal variations will be different depending on the situations of the day, e.g., human activities, the local meteorological elements, and $PM_{2.5}$ (domestic and an inflow of from abroad). On a non-event day, it ranged from 12.9 to 39.7 km with an average 22.9 km. The highest visibility appeared at around 5 p.m. and then rapidly decreased until around 3 a.m. local time. Meanwhile, during the event day, it showed a gentle time-variation with a significantly reduced value ranged 5.1–13.4 km with an average 7.9 km. The peak value occurred in the early afternoon between 1 p.m. and 2 p.m. local time and then it decreased until the morning rush hour of the next day.

Photo 1. Comparison of visual characteristics from the ground station of this study on a non-event day ($PM_{2.5}$: 21 μg/m^3) (top) and the event day (bottom) when $PM_{2.5}$ reached 63 μg/m^3.

Fig. 2 shows the time dependent variation of the visibility with the measured $PM_{2.5}$ during the event day. The environmental standard of $PM_{2.5}$ in Korea is also displayed in the figure. The visibility was determined by the ε_{sca} measured by a Nephelometer.

During the event day, the daily average mass concentration of $PM_{2.5}$ ranged from 42 to 83 μg/m^3 with an average concentration of 63 μg/m^3. The time serial $PM_{2.5}$ was severely fluctuated throughout the whole event day. Unlike non-event day, the rush-hour peak of $PM_{2.5}$ was not found. This result indicates that, added to the domestic factors including the local sources, the inflow of $PM_{2.5}$ from abroad had a significant influence on the diurnal variation of $PM_{2.5}$ on event day. This unusual hourly variation of $PM_{2.5}$ at Gwangju on the event day has also been introduced in a previous study (Park *et al.*, 2013). Meanwhile, a symmetrical temporal variation with the concentration of $PM_{2.5}$ indicates that visibility has a strong inverse proportion $PM_{2.5}$. The opposite diurnal patterns between $PM_{2.5}$ and visibility has also been measured in an urban area of Northeast China by Zhao *et al.* (2017).

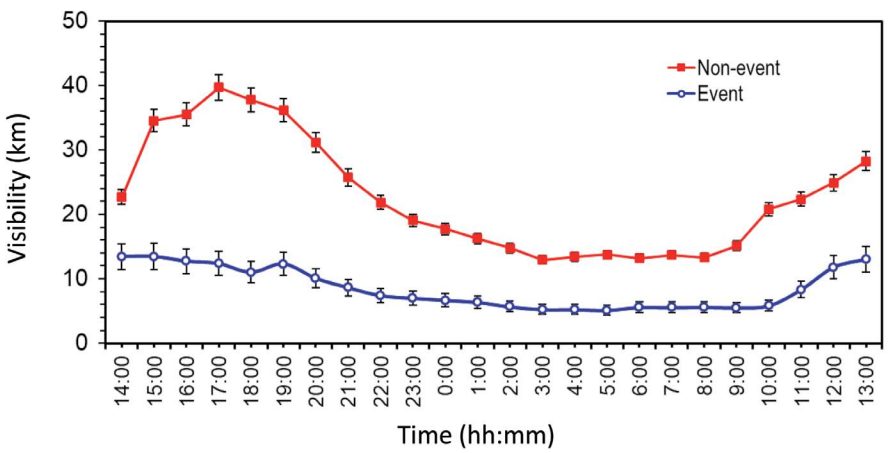

Fig. 1. Diurnal variation of visibility on the event day and a non-event day.

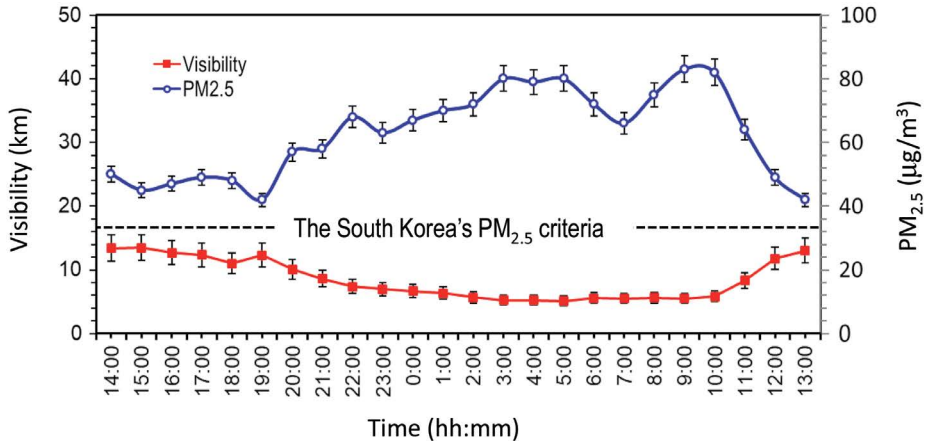

Fig. 2. Diurnal variation of visibility and $PM_{2.5}$ concentration on the event day. The South Korea's $PM_{2.5}$ criteria is the daily mean value observed every hour.

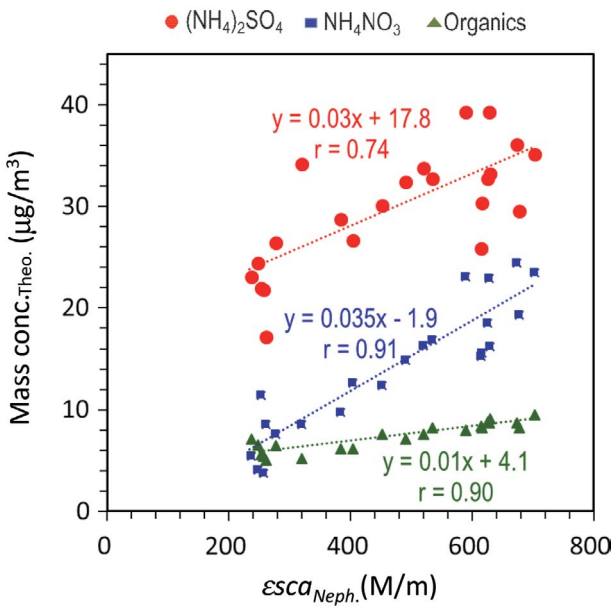

Fig. 3. Scatter plots of $\varepsilon_{sca_{Neph.}}$ and the mass concentrations of major three particle types (i.e., $(NH_4)_2SO_4$, NH_4NO_3, and organics) on the event day.

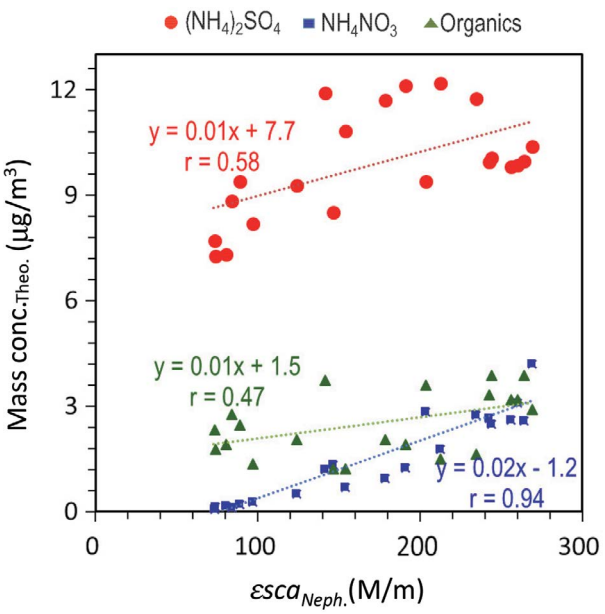

Fig. 4. Scatter plots of $\varepsilon_{sca_{Neph.}}$ and the mass concentrations of major three particle types (i.e., $(NH_4)_2SO_4$, NH_4NO_3, and organics) on a non-event day.

3.2 $\varepsilon_{sca_{Neph.}}$ and Three Kinds of Particles

To evaluate the contribution of each particle type to the ε_{sca} measured by a Nephelometer ($\varepsilon_{sca_{Neph.}}$), the scatter plots of $\varepsilon_{sca_{Neph.}}$ and the theoretically reconstructed mass concentration of major three particle types (i.e., $(NH_4)_2SO_4$, NH_4NO_3, and organics) were drawn Fig. 3 (on the event day) and Fig. 4 (on a non-event day). Sulfate was assumed to be fully neutralized (i.e., $(NH_4)_2SO_4$).

The mass concentration (m) of $(NH_4)_2SO_4$, NH_4NO_3, and organics was theoretically calculated. The m of NH_4NO_3, and $(NH_4)_2SO_4$ described as following equations was calculated from the IC results of ammonium, nitrate, and sulfate ions under assumption that the combined forms of NH_3 with nitrate and sulfate were NH_4NO_3 and $(NH_4)_2SO_4$, respectively.

$$m_{NH_4NO_3} = NO_3^-{}_{IC} \frac{NH_4NO_{3\,M.W.}}{NO_{3\,M.W.}}$$

$$m_{(NH_4)_2SO_4} = SO_4^{2-}{}_{IC} \frac{(NH_4)_2SO_{4\,M.W.}}{SO_{4\,M.W.}}$$

where $NO_3^-{}_{IC}$ and $SO_4^{2-}{}_{IC}$ are the IC results (μg/m^3) of nitrate and sulfate, respectively. *M.W.* is molecular weight.

The mass of organics, $m_{Organics}$, was determined by multiplying the amount of OC concentration (μg/m^3) by 1.6 (Cabada *et al.*, 2004; Countess *et al.*, 1980).

$$m_{Organics} : OC_{conc.} \times 1.6$$

As shown in Fig. 3, the high correlations (r values varied from 0.74 to 0.91) between the $\varepsilon_{sca_{Neph.}}$ and three particle types appeared on the event day. The high correlation coefficients, especially, with NH_4NO_3 and organics, indicate that the nitrate and organic compounds dominantly contributed to the light scattering in Gwangju during $PM_{2.5}$ event day. The similar results have been obtained in the studies carried out in the urban sites of Taiwan (Kuo *et al.*, 2013) and China (Yu *et al.*, 2019). These studies suggested that the visibility degradation due to nitrate was much higher than that due to sulfate. However, these results are a little bit different from that of Detroit's summertime atmosphere reported by Wolff *et al.* (1982). They suggested that sulfate was the most efficient light-scattering species per unit mass of dry weight.

According to the study conducted by Tao *et al.* (2007) in Guangzhou, China, the correlation coefficients of sulfate, nitrate, and OC between visibility were −0.66, −0.64, and −0.63, respectively. Jung *et al.* (2009) also reported that $(NH_4)_2SO_4$, NH_4NO_3, and organics contributed 42.2%, 24.9%, and 9.0% of light extinction coefficient (b_{ext}) in Beijing during the maximum polluted period in 2006.

Although there were slight differences in contribution rates in various studies reported previously, there is no doubt that the major secondary particles contribute greatly to visibility deterioration.

Meanwhile, as shown in Fig. 4, the $\varepsilon_{sca_{Neph.}}$ has a strong correlation ($r = 0.94$) with only NH_4NO_3 in the non-event day. However, a related study carried out by Yu *et al.* (2019) in an urban-industrial site in China during the recent wintertime suggested that sulfate was the largest contributor for the clean period. The results in Fig. 4 also indicate that there was no apparent correlation between OM and the $\varepsilon_{sca_{Neph.}}$ ($r = 0.47$) on a non-event day.

3.3 Interrelationships among Particle Components, Meteorological factors, and Visibility

The interrelationships among components (visibility, sulfate, nitrate, OC, EC, temperature (Temp.), wind speed (W.S.), relative humidity (Rh), and $PM_{2.5}$) on the event day were analyzed (Fig. 5). The visibility on the event day had negative correlations with $PM_{2.5}$, PM_{10}, nitrate, relative humidity, EC, OC, and sulfate. Especially, $PM_{2.5}$ and PM_{10} showed fairly strong negative correlation coefficients of −0.76 and −0.73 with visibility. Meanwhile, visibility had a slightly high correlation coefficient with temperature ($r = 0.65$) and wind speed ($r = 0.59$), while it has a negative correlation with relative humidity ($r = -0.58$). This result is remarkably consistent with that of Xue *et al.* (2015). Xue *et al.* (2015) reported that the visibility of Shanghai reached about 25 km at a time when temperature and wind speed were high, while visibility decreased to 16 km under the weather type of low wind speed and temperature, and high relative humidity. High temperature can promote the dispersion of the air pollutants, as a result, cause higher visibility. High wind leads to unstable meteorological conditions which accelerate the dispersion of pollutants, and then contribute to improved visibility. High relative humidity can induce the increasing of PM concentration because aerosol hygroscopic increases significantly. Finally, the increasing of PM, especially $PM_{2.5}$, can induce the aerosol scattering capability and the visibility decreasing.

3.4 Visibility Forecasting Model Based on the Routinely Collected Measurement Data

Ann *et al.* (2000) reported that visibility showed strong seasonal fluctuations in Seoul, Korea with the worst in spring. According to their study, visibility was less than 10 km in Seoul on most days of spring. Therefore, if it is possible to easily predict the visibility even in spring, it will be very helpful in our daily lives.

In this study, a simple visibility forecasting model was constructed by a statistical approach. The advantage of our model is that it does not require special observations using professional measuring devices to obtain the data needed to build the model. Our statistical model is based on the routinely monitored $PM_{2.5}$ and meteorological data from the ambient air monitoring stations widely distributed throughout the country.

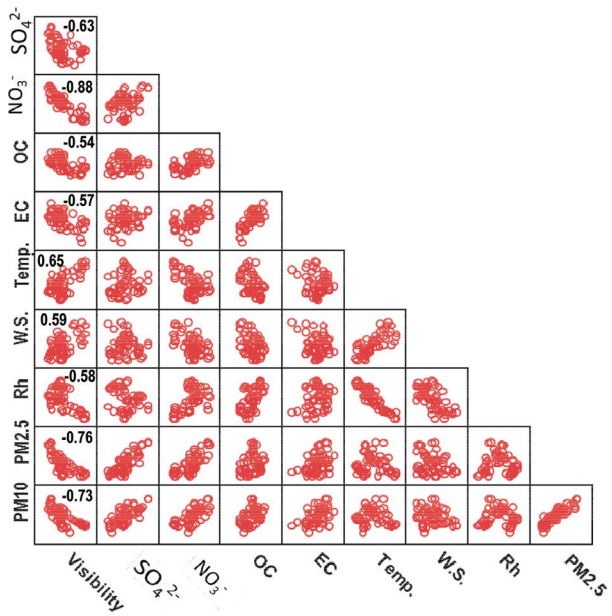

Fig. 5. The interrelationships among components (visibility, sulfate, nitrate, OC, EC, temperature (Temp.), wind speed (W.S.), relative humidity (Rh), and $PM_{2.5}$) on the event day. The numbers in plots mean Pearson's correlation coefficiency.

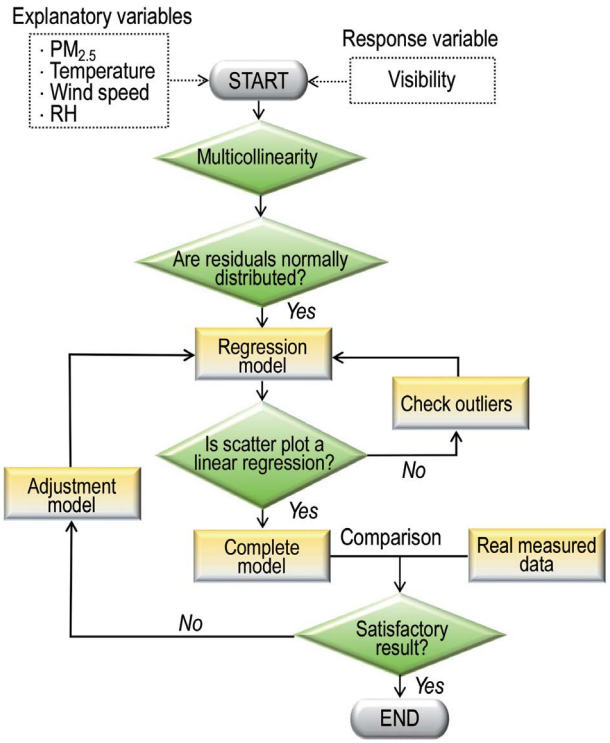

Fig. 6. Flowchart for multi step regression model with step-wise induction of variables.

3.4.1 Multicollinearity Test among Explanatory Variables

Fig. 6 shows the statistical procedure for the multi-step regression model with step-wise induction of variables. $PM_{2.5}$, temperature, wind speed, and relative humidity data were selected as the explanatory variables. These data can be taken in routinely from the Honam area air pollution intensive monitoring site in Gwangju Metropolitan City.

At first, in order to check the multicollinearity among explanatory variables, a multicollinearity index known as the variance inflation factor (*VIF*) was calculated by the following equation (Hossain *et al.*, 2010):

$$VIF_i = \frac{1}{1-R_i^2}, i = 1,2,\ldots,n.$$

where n is the number of predictor variables and R^2_i is the square of the multiple correlation coefficient of the i th variable with the remaining $(n-1)$ variables.

If *VIF* ranges from 0 to 5, there is not the multicollinearity problem (Hossain *et al.*, 2010). The calculated *VIF*s among the combination of four explanatory variables are listed in Table 1 and they varied from 1.00 to 1.03. It can therefore be said that there is no correlation among four selected explanatory variables.

3.4.2 The Built Model Formula

The coefficients for four kinds explanatory variables determined by a multi-step regression model are also listed in Table 1. The constructed visibility forecasting model was as follow:

$$Visibility\ (\text{km}) = 29.562 - 0.268\ PM_{2.5} + 0.211\ Temp. + 0.161\ Wind\ speed - 0.072\ RH$$

As expected, the constructed model suggests that $PM_{2.5}$ is the most important contributor to worsening visibility. Among the three potential meteorological variables, temperature is the most influential factor in determining the visibility reduction. Our model also indicates that wind speed, along with temperature, contributes to the improvement of visibility. This may seem reasonable because the wind plays a major role in spreading pollutants. Meanwhile, relative humidity, as shown already in Fig. 5, has a role to play in reducing visibility.

The impact of meteorology on visibility was also revealed in the field study conducted in Shanghai, China by Xue *et al.* (2015). They reported that visibility was reduced to 16 km under the weather condition of low wind speed and temperature, and high relative humidity.

Table 1. The coefficients for four kinds variables by multi step regression model.

Model	Unstandardized coefficients		Standardized coefficients	t	Sig.	VIF
	B	Std. Error	Beta			
Constant	29.562	0.92		8.57	0.00	
$PM_{2.5}$	−0.268	0.02	−0.88	−12.73	0.00	1.03
Temperature	0.211	0.10	−0.06	4.64	0.65	1.00
Wind speed	0.161	0.45	−0.10	2.52	0.28	1.01
Relatve humidity	−0.072	0.02	−0.46	−4.34	0.00	1.00

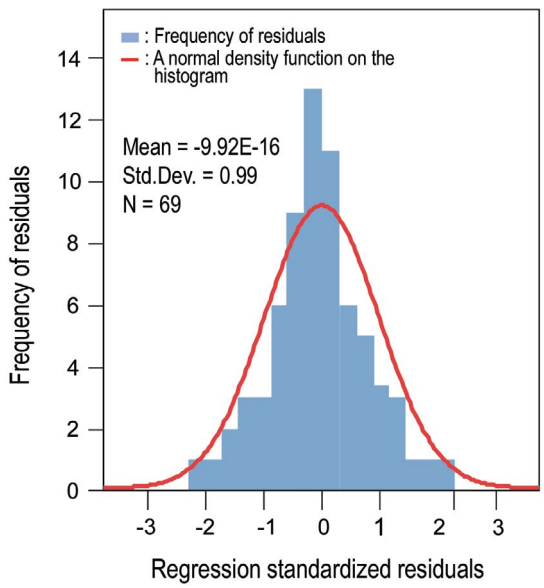

Fig. 7. Approximately normal distribution of standardized residuals produced by a model for a calibration process.

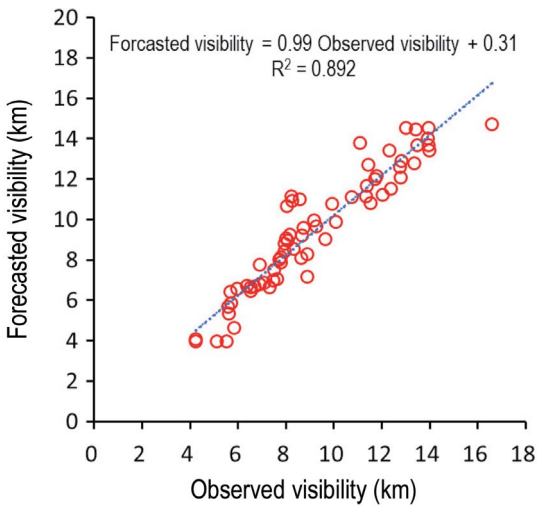

Fig. 8. Scatter plot of the observed and forecasted visibilities.

3.4.3 Test for Residual Normality

A residual plot check is a key part of next steps after model-building. Here, the residual means the values for the difference between the observed data and the predicted data. Examining residual normality suggests that the assumptions were reasonable in the process of building the model and that the model selection was appropriate. In general, the overall pattern of the residuals should be normally distributed.

As shown in Fig. 7, the bell-shaped frequency of regression standardized residuals with a normal density function on the histogram indicates that the model built in this study is very reasonable.

3.4.4 Model Validation

To validate the built model in this study, the predicted visibilities by model were compared with those of actually observed at the Gwangju Regional Meteorological Administrations (GRMA). The GRMA (35.17N; 126.89E) is about 9 km away from the Honam area air pollution intensive monitoring site.

Fig. 8 shows the scatter plot of the observed and predicted visibilities with a dotted regression line. A very high correlation ($r^2 = 0.892$) between the observed and predicted visibilities has been proved. It can therefore be said that the model designed in this study can predict visibility with accuracy, and predicted results can be useful in our daily lives.

4. CONCLUSIONS

The results of this study verified that a high $PM_{2.5}$ mass concentration is one of the important factors in the deterioration of visibility once again. The visibility

during $PM_{2.5}$ episode was also closely linked to particle kinds, specially the fine secondary particles. Through the correlation analysis between the measured ε_{sca} by a Nephelometer and the theoretically reconstructed mass concentration of three major types of particles, it can be concluded that NH_4NO_3 and organics dominantly contributed to light scattering during the $PM_{2.5}$ event day in Gwangju. Although a large amount of measured data must be used to build a good regression prediction model, the model built in this study used the monitored data over a limited period of spring. Therefore, it is not reasonable to predict the visibility of the whole season. However, it is expected that our results will contribute to establishing measures for our daily life by predicting visibility during the springtime when episodically high $PM_{2.5}$ concentrations are often observed.

ACKNOWLEDGEMENT

This study was supported in part the study on the source contribution of pollutants and the characteristics of regional air parcel movement in the Korean Peninsula (II).

REFERENCES

Anderson, T.L., Ogren, J.A. (1998) Determining aerosol radiative properties using the TSI 3563 Integrating Nephelometer. Aerosol Science and Technology, 29(1), 57–69. https://doi.org/10.1016/S0021-8502(97)00460-6

Ann, M.J., Yoon, J.S., Jo, S.J., Yeo, I.H., Lee, M.H., Kim, M.Y. (2000) Seasonality and relation to atmospheric characteristics in Visibility. Proceedings of the Korea Air Pollution Research Association Conference, 361–362.

Beccaceci, S., McGhee, E.A., Brown, B.J.C., Green, D.C. (2015) A comparison between a semi-continuous analyzer and filter-based method for measuring anion and cation concentrations in PM_{10} at an urban background site in London. Aerosol Science and Technology, 49(9), 793–801. https://doi.org/10.1080/02786826.2015.1073848

Bodhaine, B.A., Ahlquist, N.C., Schnell, R.C. (1991) Three wavelength nephelometer suitable for aircraft measurement of background aerosol scattering coefficient. Atmospheric Environment, 25A, 2267–2276. https://doi.org/10.1016/0960-1686(91)90102-D

Cabada, J.C., Khlystov, A., Wittig, A.E., Pilinis, C., Pandis, S.N. (2004) Light scattering by fine particles during the Pittsburgh Air Quality Study: Measurements and modeling. Journal of Geophysical Research, 109, D16S03. https://doi.org/10.1029/2003JD004155

Countess, R.J., Wolff, G.T., Cadle, S.H. (1980) The Denver winter aerosol: a comprehensive chemical characterization. Journal of the Air Pollution Control Association, 30, 1194–1200. https://doi.org/10.1080/00022470.1980.10465167

Gwangju Regional Meteorological Administrations, [(accessed on 19 March 2020)] Available online: https://data.kma.go.kr/data/grnd/selectAsosRltmList.do?pgmNo=36&tabNo=1

Hansen, A.D.A., Rosen, H., Novakov, T. (1982) Real-time measurement of the absorption coefficient of aerosol particles. Applied Optics, 21, 3060–3062. https://doi.org/10.1364/AO.21.003060

He, X., Li, C., Lau, A., Deng, Z., Mao, J., Wang, M., Liu, X. (2009) An intensive study of aerosol optical properties in Beijing urban area. Atmospheric Chemistry and Physics, 9, 8903–8915. https://doi.org/10.5194/acp-9-8903-2009

Hossain, M.G., Sabiruzzaman, M., Islam, S., Ohtsuki, F., Lestrel, P.E. (2010) Effect of craniofacial measures on the cephalic index of Japanese adult female students. Anthropological Science, 118(2), 117–121.

Jung, J., Lee, H., Kim, Y.J., Liu, X., Zhang, Y., Hu, M., Sugimoto, N. (2009) Optical properties of atmospheric aerosols obtained by in situ and remote measurements during 2006 Campaign of Air Quality Research in Beijing (CAREBeijing-2006). Journal of Geophysical Research, 114, D00G02. https://doi.org/10.1029/2008JD010337

Karanasiou, A., Minguillón, M.C., Viana, M., Alastuey, A., Putaud, J.-P., Maenhaut, W., Panteliadis, P., Mocnik, G., Favez, O., Kuhlbusch, T.A.J. (2015) Thermal-optical analysis for the measurement of elemental carbon (EC) and organic carbon (OC) in ambient air a literature review. Atmospheric Measurement Techniques Discussion, 8, 9649–9712. https://doi.org/10.5194/amtd-8-9649-2015

Kim, K.W., Kim, Y.J., Bang, S.Y. (2008) Summer time haze characteristics of the urban atmosphere of Gwangju and the rural atmosphere of Anmyon, Korea. Environmental Monitoring and Assessment, 141, 189–199. https://doi.org/10.1007/s10661-007-9887-8

Koschmieder, H. (1924) Theorie der horizontalen Sichtweite. Beiträge zur Physik der Atmosphäre, 12, 33e55.

Kuo, C.Y., Cheng, F.C., Chang, S.Y., Lin, C.Y., Chou, C.C., Chou, C.H., Lin, Y.R. (2013) Analysis of the major factors affecting the visibility degradation in two stations. Journal of the Air & Waste Management Association, 63(4), 433–441. https://doi.org/10.1080/10962247.2012.762813

Malm, W.C., Sisler, J.F., Huffman, D., Eldred, R.A., Cahill, T.A. (1994) Spatial and seasonal trends in particle concentration and optical extinction in the United States. Journal of Geophysical Research, 99(D1), 1347–1370. https://doi.org/10.1029/93jd02916

Park, S.S., Jung, S.A, Gong, B.J., Cho, S.Y., Lee, S.J. (2013) Characteristics of $PM_{2.5}$ haze episodes revealed by highly time-resolved measurements at an air pollution monitoring supersite in Korea. Aerosol and Air Quality Research, 13, 957–976.

Sloane, C.S., Watson, J.G., Chow, J.C., Pritchett, L.C., Richards, L.W. (1991) Sized-segregated fine particle measurements by chemical species and their impact on visibility impairment

in Denver. Atmospheric Environment, 25A, 1013–1024. https://doi.org/10.1016/0960-1686(91)90143-U

Tao, J., Ho, K.F., Chen, L., Zhu, L., Han, J., Xu, Z. (2009) Effect of chemical composition of $PM_{2.5}$ on visibility in Guangzhou, China, 2007 spring. Particuology, 7, 68–75. https://doi.org/10.1016/j.partic.2008.11.002

The car registration number by year (2016) http://www.kosis.kr/search/total

Wang, Y.H., Liu, Z.R., Zhang, J.K., Hu, B., Ji, D.S., Yu, Y.C., Wang, Y.S. (2015) Aerosol physicochemical properties and implications for visibility during an intense haze episode during winter in Beijing. Atmospheric Chemistry and Physics, 15, 3205–3215. https://doi.org/10.5194/acp-15-3205-2015

Watson, J.G. (2002) Visibility: Science and Regulation. Journal of the Air Pollution Control Association, 52, 628–713. https://doi.org/10.1080/10473289.2002.10470813

Wolff, G.T., Ferman, M.A., Kelly, N.A., Stroup, D.P., Ruthkosky, M.S. (1982) The relationships between the chemical composition of fine particles and visibility in the Detroit Metropolitan area. Journal of the Air Pollution Control Association, 32(12), 1216–1220. https://doi.org/10.1080/00022470.1982.10465534

Xue, D., Li, C., Liu, Q. (2015) Visibility characteristics and the impacts of air pollutants and meteorological conditions over Shanghai, China. Environmental Monitoring and Assessment, 187(6), 363. https://doi.org/10.1007/s10661-015-4581-8

Yan, P., Tang, J., Huang, J., Mao, J., Zhou, X., Liu, Q., Wang, Z., Zhou, H. (2008) The measurement of aerosol optical properties at a rural site in Northern China. Atmospheric Chemistry and Physics, 8, 2229–2242. https://doi.org/10.5194/acp-8-2229-2008

Yao, T., Huang, X., He, L., Hu, M., Sun, T., Xue, L., Lin, Y., Zeng, L., Zhang, Y. (2010) High time resolution observation and statistical analysis of atmospheric light extinction properties and the chemical speciation of fine particulates. Science China Chemistry, 53, 1801–1808. https://doi.org/10.1007/s11426-010-4006-z

Yu, X., Shen, L., Xiao, S., Ma, J., Lü, R., Zhu, B., Hu, J., Chen, K., Zhu, J. (2019) Chemical and optical properties of atmospheric aerosols during the polluted periods in a megacity in the Yangtze river delta, China. Journal of Aerosol and Air Quality Research, 19, 103–117. https://doi.org/10.4209/aaqr.2017.12.0572

Zhao, H., Che, H., Ma, Y., Wang, Y., Yang, H., Liu, Y., Wang, Y., Wang, H., Zhang, X. (2017) The relationship of PM variation with visibility and mixing-layer height under hazy/foggy conditions in the multi-cities of northeast China. International Journal of Environmental Research and Public Health, 14(5), 471. https://doi.org/10.3390/ijerph14050471